THE JOURNAL OF PHYSICAL CHEMISTRY C

Article

pubs.acs.org/JPCC

Programming Hierarchical Supramolecular Nanostructures by Molecular Design

Yeliang Wang,[†,‡] Magalí Lingenfelder,[†,○] Stefano Fabris,[§] Guido Fratesi,[§,◆] Riccardo Ferrando,[∥] Thomas Classen,[†,¶] Klaus Kern,[†,#] and Giovanni Costantini*[,†,▽]

[†]Max-Planck-Institute for Solid State Research, Heisenbergstr. 1, 70569 Stuttgart, Germany

[‡]Institute of Physics, Chinese Academy of Sciences, 100190 Beijing, People's Republic of China

[§]CNR-IOM DEMOCRITOS, Theory@Elettra Group, IOM and SISSA, via Bonomea 265, 34136,Trieste, Italy

[∥]Department of Physics, University of Genova and IMEM/CNR; Via Dodecaneso 33, 16146 Genova, Italy

[#]ICMP, Ecole Polytechnique Fédérale de Lausanne, CH-1015 Lausanne, Switzerland

[▽]Department of Chemistry, University of Warwick, Gibbet Hill Road, Coventry, CV47AL, United Kingdom

Supporting Information

ABSTRACT: Supramolecular nanostructures with tunable dimensionalities are fabricated by deposition of benzene−carboxylic acids on the Cu(110) surface. By tailoring the number and position of the functional moieties, the structure of the final molecular assemblies can be rationally modified ranging from isolated one-dimensional chains to compact two-dimensional islands. Molecular units are chosen that can assemble through metal−organic and electrostatic interactions. The hierarchy between these intermolecular forces guarantees that a primary organization level, constituted by metal−organic polymeric chains, is developed by all molecular units while the secondary interchain interactions can be arbitrarily adjusted. Scanning tunneling microscopy, density functional theory calculations, and kinetic Monte Carlo simulations are used to characterize and rationalize the experimental findings.

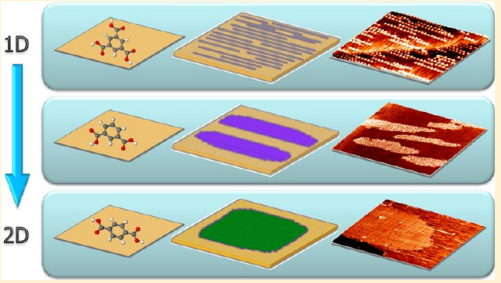

1. INTRODUCTION

Self-assembly has emerged as the only way to organize functional molecular building blocks on a length scale of few nanometers that is at the same time effective, reproducible, cheap, and thus viable to be scaled-up to mass production and, in particular, with a high degree of order and faultlessness.[1] As such, supramolecular self-assembly has become an increasingly popular approach for the formation of functional nanoarchitectures with potential use in catalysis,[2,3] gas storage,[4] magnetism,[5] and molecular electronics.[6−8] Many of the devised applications require the fabrication of ordered molecular arrays on substrates for the accessibility of the devices to an external environment and for their addressability and readout. The controlled transfer of solution-grown two-dimensional (2D) supramolecular nanostructures onto solid surfaces is challenging because of the noncovalent bonds involved in their stabilization, which might be altered by molecule−surface interactions.[9] Direct molecular self-assembly at surfaces has proven as an excellent alternative both at the solid−liquid[10] and at the solid−vacuum interface.[11] For example, porous networks capable of trapping guest molecules have been developed in this way,[12−14] functional multicomponent systems of molecular semiconductors,[15] atomically precise graphene nanoribbons,[16] and ordered arrays of high-spin centers.[17]

Although the ultimate goal of the supramolecular approach is to rationally assemble elementary components into specific structures that perform a specific function, at present, this is still far from reach,[18] in particular, for "surface-assisted" self-assembly. The complexity of the problem is such that only rarely it becomes possible to actually determine the balance between the different intermolecular and molecule−surface interactions with the consequence that most of the results are only rationalized a posteriori.

Hierarchical self-assembly, that is, "the formation of an ordered structure through a set of interactions that decreases in strength"[19] is an extremely efficient way of constructing complex functional architectures developed by nature through billions of years of evolution. A major advantage of this approach is that the formation of ordered superstructures at higher levels of organization does not dismantle but builds upon the lower-lying levels.

Inspired by nature, researchers have applied a hierarchical stepwise approach to the molecular assembly of synthetic systems, thereby attaining a much higher control and predictability of the final supramolecular arrangements. This has been particularly successful in three-dimensional (3D) solution chemistry[20,21] where, for example, it has been applied to the fabrication of DNA nanostructures[22,23] and functional

Received: September 26, 2012
Revised: December 11, 2012
Published: January 14, 2013

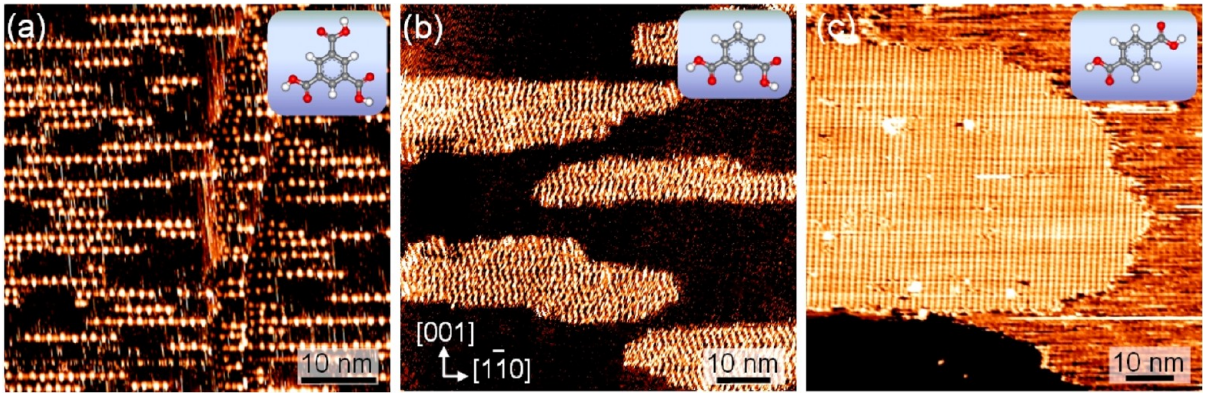

Figure 1. Supramolecular structures formed through the deposition of three planar benzene−carboxylic acids on the Cu(110) surface. (a) Separated 1D chains in the case of TMA; (b) anisotropic islands elongated along [1$\bar{1}$0] for IPA; (c) compact and extended 2D islands for TPA. The inset in each image shows the structure of the corresponding molecule. STM images acquired at a sample bias voltage U_{bias} = −1.5 V and a tunnelling current I = 0.8 nA. The scale bar corresponds to 10 nm in all images.

inorganic nanoparticle−polymer composites[24,25] or in the bioinspired mineralization of inorganic crystals.[26] Unfortunately, the situation in 2D self-assembly at surfaces is complicated by the interaction with the substrate that competes with intermolecular interactions often resulting in the loss of an actual predictive capability. Nevertheless, several 2D assemblies at surfaces have been demonstrated[27−34] that have a hierarchical structure emerging from a very complex and subtle balance of forces.

Here, we report on the use of a hierarchical approach for building surface-supported supramolecular nanostructures. We show that, by opportunely designing planar benzene−carboxylic acids, the dimensionality of metal−organic structures formed on a Cu(110) substrate can be continuously tuned from one-dimensional (1D) to 2D. All the selected molecules are able to assemble into 1D chains by coordination bonding with metal centers.[35] These chains represent the elementary units of the first complexity level and interact among each other through weaker electrostatic and hydrogen bonds that can be adjusted by molecular design.

2. EXPERIMENTAL AND COMPUTATIONAL METHODS

2.1. Experimental Details. Samples were prepared and analyzed in an ultrahigh vacuum (UHV) system providing controlled experimental conditions. The system includes a preparation chamber (base pressure of ∼2 × 10^{-10} mbar) and a variable temperature scanning tunnelling microscopy (STM) apparatus (∼5 × 10^{-11} mbar). Atomically flat and clean Cu(110) surfaces were prepared by several cycles of Ar^+ sputtering (900 eV, 10 $\mu A/cm^2$) and subsequent annealing (850 K) of a single crystal sample. Three kinds of planar benzene−carboxylic molecules, trimesic acid (1,3,5-benzenetricarboxylic acid, TMA), isophthalic acid (1,3-benzenedicarboxylic acid, IPA), and terephthalic acid (1,4-benzenedicarboxylic acid, TPA), were deposited by means of organic molecular beam epitaxy from a Knudsen-cell evaporator. The quartz crucibles were held at 460, 440, and 415 K for TMA, TPA, and IPA, respectively. The Cu(110) substrate was maintained at room temperature during deposition. A subsequent annealing to 380 K was employed only for the TMA deposition. The sample temperature was measured by a K-type thermocouple connected to the back of the Cu crystal. STM measurements were performed in the constant-current mode with electrochemically etched tungsten tips. Voltages are referred to the sample; negative bias thus implies occupied states imaging.

2.2. Computational Details: Density Functional Theory (DFT) Calculations. The DFT calculations employed the generalized gradient corrected approximation of Perdew−Burke−Ernzerhof for the exchange and correlation energy.[36] The calculations were performed in the pseudopotential plane-wave framework (plane-wave basis-set for wave function and density representation limited by a cutoff of 24 and 200 Ry, respectively) using ultrasoft pseudopotentials[37] as implemented in the PWscf code of the Quantum-Espresso simulation package.[38] Brillouin zone integrals were calculated on regular meshes generated with the Monkhorst and Pack[39] grids equivalent to or denser than the (9 6 1) one for the primitive 1 × 1 supercell of the Cu(110) surface, together with a Gaussian smearing of 0.2 eV. A three-layer supercell slab separated by 10 Å of vacuum provided a simplified model of the Cu(110) surface. The atomic positions were determined by relaxing the upper layer and keeping the distance between the others fixed at the bulk value. Copper adatoms and deprotonated carboxylate molecules were positioned on the upper surface of the slab and were structurally relaxed according to the Hellmann−Feynman forces. STM images were simulated by means of the Tersoff−Hamann method,[40] that is, by a spatially resolved DOS integrated in energy from a bias potential (−1.0 eV) to the Fermi energy. The intra- and interchain molecular interactions are calculated in terms of total energy differences of the (Cu−molecule−Cu) units isolated or assembled on the Cu(110) surface.

2.3. Computational Details: Kinetic Monte Carlo (KMC) simulations. Simulations of the supramolecular self-assembly were based on the KMC method. The initial configuration corresponded to a random distribution of the molecules on a discrete 50 × 50 grid. The coverage, the annealing temperature, and the annealing time were identical to the experimental conditions. An anisotropic bond-breaking model was employed to reproduce the two major intermolecular interactions: stronger metal−organic bonding along [1$\bar{1}$0] and weaker electrostatic repulsion/attraction along [001]. The model was made by trying to adopt the most simplifying assumptions and using the available information from DFT calculations. Thermally activated diffusion was reproduced by allowing each molecule to hop into one of the unoccupied neighboring lattice sites with an Arrhenius-like rate.

dx.doi.org/10.1021/jp309566s | J. Phys. Chem. C 2013, 117, 3440−3445

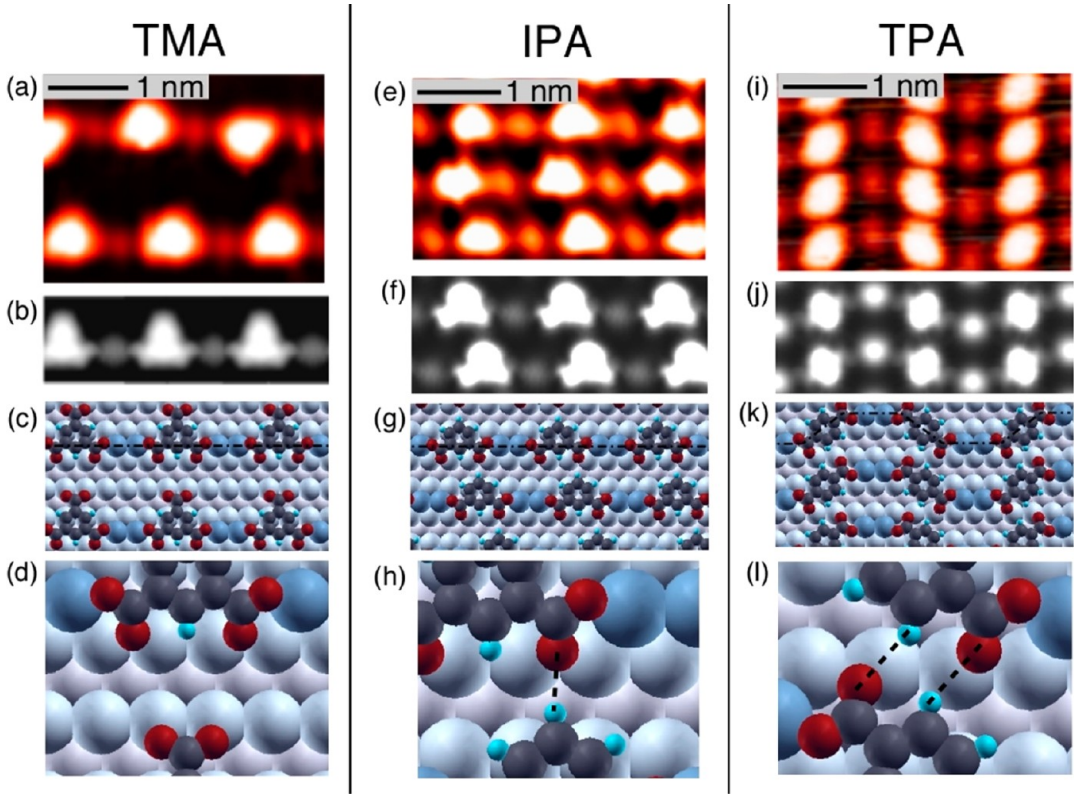

Figure 2. Metal−organic $[-Cu-molecule-Cu-]_n$ chains. High-resolution STM images (a, e, i). DFT lowest energy configurations (b, f, j) and corresponding DFT simulated images (c, g, k). Details of the interchain interactions (d ,h ,l). The dash-dotted lines illustrate the shape of the metal−organic chains. Dashed lines in (h) and (l) depict the H bonds. STM images acquired at −1.0 V, 1.0 nA in (a), −1.5 V, 0.8 nA in (e), and −1.6 V, 0.5 nA in (i).

The diffusion barriers of isolated molecules were chosen to be identical along the two principal crystallographic directions, but their values were specific to the different molecules. The specific detailed values of the simulation parameters are contained in the Supporting Information.

3. RESULTS AND DISCUSSION

Previous studies on the adsorption of carboxylic acids onto metallic substrates have revealed that, in particular on copper, the [COOH] groups deprotonate to produce highly reactive carboxylate [COO^-] moieties at (or above) room temperature.[41−45] These may bind with metal atoms either from the substrate or intentionally codeposited, thus generating metal−organic complexes[46−48] stabilized by genuine coordination interactions.[49]

In the case of TMA on Cu(110), these effects cooperate with the templating action of the anisotropic substrate[35,50] to determine the unidirectional and separated metal−organic chains observed in Figure 1a. High-resolution STM images reveal that an individual chain is constituted by alternating flat-laying TMA molecules (brighter triangular protrusions) and Cu dimers (darker rounded protrusions)[35] with a periodicity of five Cu lattice spacings along $[1\bar{1}0]$ (Figure 2a). DFT calculations performed for this system yield simulated STM images that are in good agreement with the experimental data (Figure 2b). The lowest-energy configuration corresponds to chains stabilized by the binding of two carboxylate groups in each TMA molecule with Cu dimers, so as to form 1D $[-Cu-TMA-Cu-]_n$ coordination polymers along the $[1\bar{1}0]$ direction (Figure 2c). The remaining carboxylate groups point out of the chains, randomly up or down. The electrostatic repulsion between these [COO^-] "tips" and molecules in neighboring chains causes the observed separation. Although the theoretical minimum interchain distance is of three lattice spacings along [001] (Figure 2c), most of the times a larger value is observed, due to the repulsion between two accidentally facing "tips" (right side of Figure 2a). However, even at a high molecular coverage, kinks are never seen within a chain, clearly indicating the relative strength of the intrachain coordinative binding that privileges a straight chain arrangement. Indeed, our DFT calculations predict the intrachain interaction to be attractive (−0.27 eV) while the interchain interaction to be more than an order of magnitude smaller.

Since the interaction between the negatively charged carboxylate groups is responsible for the separation of the metal−organic chains, we considered reducing the chain−chain repulsion by "eliminating" the third carboxylic moiety from the TMA molecule. This results in the IPA molecule, schematically depicted in the inset of Figure 1b. STM measurements show that, when IPA is deposited on Cu(110), asymmetrically $[1\bar{1}0]$ elongated islands with an aspect ratio of (3.5 ± 1.2) are formed instead of single isolated chains (Figure 1b). However, higher-resolution images evidence that the islands are still constituted of $[1\bar{1}0]$-oriented chains that, also in this case, show an alternation of brighter (nearly triangularly shaped) and darker protrusions (Figure 2e). On the basis of the simulated STM images (Figure 2f), the brighter features are assigned to planar IPA molecules and the darker protrusions to Cu dimers. The periodicity within a chain is ∼12.8 Å, thus again five Cu lattice spacings along $[1\bar{1}0]$, while the chain−chain distance is reduced

dx.doi.org/10.1021/jp309566s | J. Phys. Chem. C 2013, 117, 3440−3445

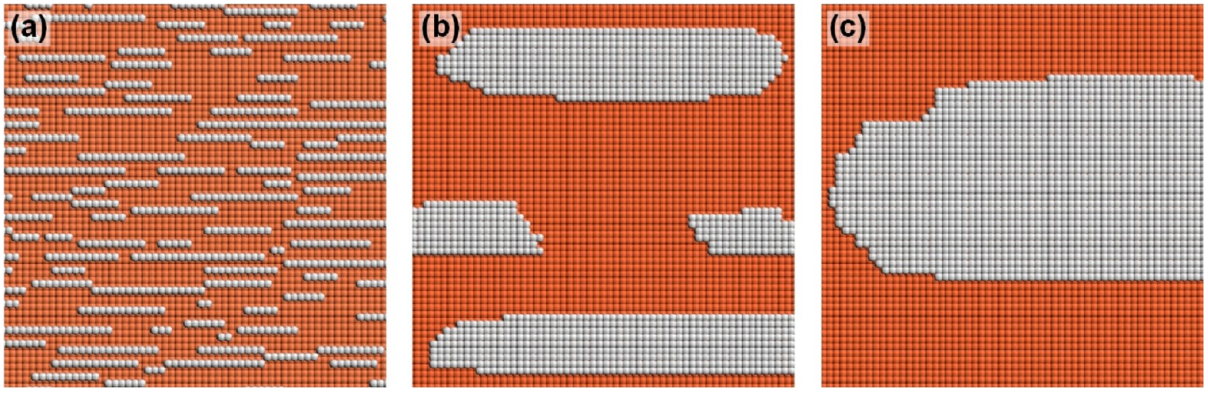

Figure 3. KMC simulations of the supramolecular structures formed on Cu(110) by (a) TMA, (b) IPA, and (c) TPA. The number of molecules, the sample temperatures, and the size are set to the same experimental conditions used for the images in Figure 1. The *x* and *y* horizontal and vertical directions correspond to the crystallographic $[1\bar{1}0]$ and [001] orientations of the Cu(110) surface, respectively. The snapshots show only a part of the entire simulation box. Details of the simulation parameters can be found in the Supporting Information.

to ∼7.2 Å, that is, two Cu lattice spacings along [001]. Adjacent $[-\text{Cu}-\text{IPA}-\text{Cu}-]_n$ chains are mutually shifted by one Cu lattice spacing in the $[1\bar{1}0]$ direction. The calculated equilibrium adsorption geometry reveals that this is because the H-atom terminal of one IPA molecule can bind to the carboxylate group of either its left or right neighbor (Figure 2h). The two configurations are degenerate in energy, which is reflected in the equal frequency of left or right shifts obtained from a statistical analysis of a large number of STM images.

The DFT results indeed prove that the primary organization level is quite insensitive to the hydrogen atom replacing one of the TMA carboxylic groups: the lowest energy configuration is still characterized by polymeric $[-\text{Cu}-\text{IPA}-\text{Cu}-]_n$ chains (Figure 2g) with an intrachain IPA binding of −0.30 eV, almost the same value obtained for TMA. On the contrary, the absence of a third carboxylic group in the IPA molecule modifies the interchain interactions (secondary organization level), which in this case, is weakly attractive. On the basis of the DFT calculations, we estimate the interaction between the $[-\text{Cu}-\text{IPA}-\text{Cu}-]_n$ chains to be ∼0.1 eV stronger than between the $[-\text{Cu}-\text{TMA}-\text{Cu}-]_n$ chains. This is because the electrostatic repulsion between opposite facing deprotonated TMA molecules is substituted by C−H···O hydrogen bonding between IPA molecules (Figure 2h). The length of this bond can be evaluated by considering the supramolecular periodicity measured by STM and the interatomic separations within a single molecule from the DFT calculations. This results in a donor to acceptor distance of 2.5 Å, which is compatible with a weak hydrogen bond as classified by Jeffrey.[51,52] The experimental observation that the primary metal−organic binding motif is preserved upon modification of the molecular building block is thus quantitatively rationalized by DFT as resulting from the hierarchy between intra- and interchain interactions.

A further strengthening of the chain−chain attractive interaction can be obtained by increasing the number of hydrogen bonds per unit chain length, that is, by "moving" the second carboxylic group of IPA from the *meta* to the *ortho* position. This implies switching from IPA to its isomer TPA (inset of Figure 1c). If TPA molecules are used as elementary building blocks for self-assembly, STM measurements show the formation of compact and extended 2D islands on the Cu(110) surface (Figure 1c). Close-up images demonstrate that the microscopic structure of these supramolecular arrangements consists of alternating brighter and darker protrusions having a periodicity of five substrate lattice spacings along $[1\bar{1}0]$ (Figure 2i). By comparison with simulated images obtained from DFT calculations (Figure 2j), these features can again be assigned to flat-lying TPA molecules and Cu dimers, respectively.[53] Thus, the same metal−organic $[-\text{Cu}-\text{TPA}-\text{Cu}-]_n$ structure is found also here as the primary assembly unit. The only difference is that the optimal matching with the Cu(110) lattice forces TPA to absorb in a geometry rotated by ±40° with respect to the substrate $[1\bar{1}0]$ direction. As a consequence, the primary metal−organic chains now have a zigzag arrangement, as denoted by the dash-dotted line in Figure 2k. The DFT calculations show that the intrachain bonding in the primary assembly is again comparable to the TMA and IPA cases (−0.31 eV). On the other hand, the interchain interaction responsible for the secondary assembly occurs through double C−H···O bonds between neighboring TPA molecules (Figure 2l, bond length 2.57 Å). It should be noted that the relative position of TPA molecules in adjacent chains determines a perfect phase matching of the $[-\text{Cu}-\text{TPA}-\text{Cu}-]_n$ chains along [001] (Figures 1c and 2i).

The supramolecular arrangements obtained through the self-assembly of TMA, IPA, and TPA on Cu(110) have the common characteristic of being composed by metal−organic chains stabilized by strong coordination bonding. These chains represent the first level of hierarchical assembly and can on their turn be employed as elementary units at a successive organization level. In particular, the interaction between the chains is mediated by electrostatic repulsion or hydrogen bonding that is weak enough not to modify the primary structures. These interactions can be adjusted by changes in the functional moieties of the molecular building blocks. Provided the molecules retain their ability to form lateral coordination bonds, the hierarchy of the intermolecular forces guarantees the possibility to modify the secondary organization level while leaving the primary unaltered.

In order to verify the generality of our approach, we performed KMC simulations of the formation process of the different supramolecular structures. A very simple KMC model was employed, with a square substrate lattice (with *x* and *y* directions corresponding to $[1\bar{1}0]$ and [001], respectively), isotropic molecular diffusion barriers, and anisotropic binding energies within and among the molecular chains.[54] Despite the extremely simple assumptions of the model, the KMC

dx.doi.org/10.1021/jp309566s | J. Phys. Chem. C 2013, 117, 3440−3445

simulations allowed reproduction of the main features of the self-assembled supramolecular structures (Figure 3) with a remarkable qualitative agreement in terms of the spatial distribution of the elementary building blocks and the dimensionality and shape of their aggregates (Figure 1). The parameter set employed in these simulations that better reproduces the experimental shape of the TPA, IPA, and TPA assemblies is reported in the Supporting Information. These parameters have a well-defined physical interpretation and provide insights into the factors governing the different supramolecular arrangements. In particular they show the following: (i) the metal−organic binding strength within the chains along the [1$\bar{1}$0] direction is the same for the three molecular nanostructures (of the order of some hundreds of millielectronvolts), in agreement with the predictions of the DFT calculations; (ii) the interaction between chains along the [001] direction is significantly smaller than the intrachain bonding (about 1 order of magnitude, as predicted by the DFT calculations) and is weakly repulsive for TMA and weakly attractive for IPA and TPA; and (iii) the smallest barrier for molecular diffusion is for TPA, and the largest is for TMA. The KMC simulations thus corroborate the energetics of the DFT calculations and help us in understanding which factors determine the different island shapes and sizes.

These results suggest that the physical parameters governing the morphology of the observed supramolecular assemblies are actually quite simple and do not depend on the fine details of the molecular structures. In particular, the transition from linear chains to anisotropic 2D aggregates and to compact 2D aggregates is ruled by the relative strength of intermolecular bonding between the primary and secondary assemblies, along the [1$\bar{1}$0] and [001] directions, respectively. This is analogous to what is found in the case of much simpler systems,[55,56] showing that the growth behavior of complex molecules can be predicted in rather simple terms.

4. CONCLUSION

In conclusion, we have demonstrated the fabrication of surface-supported supramolecular nanostructures with tunable dimensionalities. This has been possible thanks to a hierarchical approach steered by molecular design. Three different molecules were used that are able to self-assemble into 1D metal−organic polymeric chains with the same [−metal−molecule−metal−] basic unit. These chains act as elementary units for the secondary organization level where the interchain interaction was tuned in order to obtain the desired dimensionality of the final arrangements.

The ultimate goal would be to start from the KMC simulations, infer the necessary binding schemes, design and synthesize the corresponding molecular building blocks, and finally, produce the actual nanostructures. Although this might not always be straightforward, the results presented here demonstrate that a hierarchical approach represents one of the best strategies in this direction.

■ ASSOCIATED CONTENT

Supporting Information

Detailed information on the simulation parameters used in the KMC simulations. This material is available free of charge via the Internet at http://pubs.acs.org.

■ AUTHOR INFORMATION

Corresponding Author

*Phone: +44-(0)24-765-24934; fax: +44-(0)24-765-24112; e-mail: g.costantini@warwick.ac.uk.

Present Addresses

○ICMP, Ecole Polytechnique Fédérale de Lausanne, CH-1015 Lausanne, Switzerland.

◆Department of Material Sciences, University of Milano-Bicocca, via Cozzi 53, 20125 Milano, Italy.

¶Robert Bosch GmbH, Germany.

Notes

The authors declare no competing financial interest.

■ ACKNOWLEDGMENTS

We gratefully acknowledge N. Lin for fruitful discussions and S. Rauschenbach for technical assistance. Y.W. acknowledges the Alexander von Humboldt Foundation and the National Natural Science Foundation of China (NSFC) for financial support through grant number 61222112.

■ REFERENCES

(1) Lehn, J. M. *Science* **2002**, *295*, 2400−2403.
(2) Claridge, S. A.; Castleman, A. W., Jr.; Khanna, S. N.; Murray, C. B.; Sen, A.; Weiss, P. S. *ACS Nano* **2009**, *3*, 244−255.
(3) Koblenz, T. S.; Wassenaar, J.; Reek, J. N. H. *Chem. Soc. Rev.* **2008**, *37*, 247−262.
(4) Chen, B.; Xiang, S.; Qian, G. *Acc. Chem. Res.* **2010**, *43*, 1115−1124.
(5) Jain, R.; Kabir, K.; Gilroy, J. B.; Mitchell, K. A. R.; Wong, K.-C.; Hicks, R. G. *Nature* **2007**, *445*, 291−294.
(6) Meijer, E. W.; Schenning, A. *Nature* **2002**, *419*, 353−354.
(7) Keren, K.; Berman, R. S.; Buchstab, E.; Sivan, U.; Braun, E. *Science* **2003**, *302*, 1380−1382.
(8) Zang, L.; Che, Y.; Moore, J. S. *Acc. Chem. Res.* **2008**, *41*, 1596−1608.
(9) Bauer, T.; Zheng, Z.; Renn, A.; Enning, R.; Stemmer, A.; Sakamoto, J.; Schlueter, A. D. *Angew. Chem., Int. Ed.* **2011**, *50*, 7879−7884.
(10) Elemans, J. A. A. W.; Lei, S.; De Feyter, S. *Angew. Chem., Int. Ed.* **2009**, *48*, 7298−7332.
(11) Barth, J. V.; Costantini, G.; Kern, K. *Nature* **2005**, *437*, 671−679.
(12) Blunt, M. O.; Russell, J. C.; Gimenez-Lopez, M. d. C.; Taleb, N.; Lin, X.; Schroder, M.; Champness, N. R.; Beton, P. H. *Nat. Chem.* **2011**, *3*, 74−78.
(13) Stepanow, S.; Lingenfelder, M.; Dmitriev, A.; Spillmann, H.; Delvigne, E.; Lin, N.; Deng, X. B.; Cai, C. Z.; Barth, J. V.; Kern, K. *Nat. Mater.* **2004**, *3*, 229−233.
(14) Bonifazi, D.; Mohnani, S.; Llanes-Pallas, A. *Chem.—Eur. J.* **2009**, *15*, 7004−7025.
(15) MacLeod, J. M.; Ivasenko, O.; Fu, C.; Taerum, T.; Rosei, F.; Perepichka, D. F. *J. Am. Chem. Soc.* **2009**, *131*, 16844−16850.
(16) Cai, J.; Ruffieux, P.; Jaafar, R.; Bieri, M.; Braun, T.; Blankenburg, S.; Muoth, M.; Seitsonen, A. P.; Saleh, M.; Feng, X.; et al. *Nature* **2010**, *466*, 470−473.
(17) Gambardella, P.; Stepanow, S.; Dmitriev, A.; Honolka, J.; de Groot, F. M. F.; Lingenfelder, M.; Sen Gupta, S.; Sarma, D. D.; Bencok, P.; Stanescu, S.; et al. *Nat. Mater.* **2009**, *8*, 189−193.
(18) Ariga, K.; Hill, J. P.; Lee, M. V.; Vinu, A.; Charvet, R.; Acharya, S. *Sci. Technol. Adv. Mater.* **2008**, *9*, 014109.
(19) Choi, I. S.; Bowden, N.; Whitesides, G. M. *Angew. Chem., Int. Ed.* **1999**, *38*, 3078−3081.
(20) Elemans, J.; Rowan, A. E.; Nolte, R. J. M. *J. Mater. Chem.* **2003**, *13*, 2661−2670.
(21) Weiss, P. S. *ACS Nano* **2008**, *2*, 1085−1087.

(22) Goodman, R. P.; Schaap, I. A. T.; Tardin, C. F.; Erben, C. M.; Berry, R. M.; Schmidt, C. F.; Turberfield, A. J. *Science* **2005**, *310*, 1661−1665.
(23) He, Y.; Ye, T.; Su, M.; Zhang, C.; Ribbe, A. E.; Jiang, W.; Mao, C. *Nature* **2008**, *452*, 198−202.
(24) Lin, Y.; Boker, A.; He, J. B.; Sill, K.; Xiang, H. Q.; Abetz, C.; Li, X. F.; Wang, J.; Emrick, T.; Long, S.; et al. *Nature* **2005**, *434*, 55−59.
(25) Lopes, W. A.; Jaeger, H. M. *Nature* **2001**, *414*, 735−738.
(26) Yu, S. H.; Colfen, H. *J. Mater. Chem.* **2004**, *14*, 2124−2147.
(27) Spillmann, H.; Dmitriev, A.; Lin, N.; Messina, P.; Barth, J. V.; Kern, K. *J. Am. Chem. Soc.* **2003**, *125*, 10725−10728.
(28) Blum, M. C.; Cavar, E.; Pivetta, M.; Patthey, F.; Schneider, W. D. *Angew. Chem., Int. Ed.* **2005**, *44*, 5334−5337.
(29) Katano, S.; Kim, Y.; Matsubara, H.; Kitagawa, T.; Kawai, M. *J. Am. Chem. Soc.* **2007**, *129*, 2511−2515.
(30) Ecija, D.; Seufert, K.; Heim, D.; Auwaerter, W.; Aurisicchio, C.; Fabbro, C.; Bonifazi, D.; Barth, J. V. *ACS Nano* **2010**, *4*, 4936−4942.
(31) Liu, J.; Chen, T.; Deng, X.; Wang, D.; Pei, J.; Wan, L.-J. *J. Am. Chem. Soc.* **2011**, *133*, 21010−21015.
(32) Tahara, K.; Yamaga, H.; Ghijsens, E.; Inukai, K.; Adisoejoso, J.; Blunt, M. O.; De Feyter, S.; Tobe, Y. *Nat. Chem.* **2011**, *3*, 714−719.
(33) Staniec, P. A.; Perdigao, L. M. A.; Saywell, A.; Champness, N. R.; Beton, P. H. *ChemPhysChem* **2007**, *8*, 2177−2181.
(34) Yang, Y.; Wang, C. *Chem. Soc. Rev.* **2009**, *38*, 2576−2589.
(35) Classen, T.; Fratesi, G.; Costantini, G.; Fabris, S.; Stadler, F. L.; Kim, C.; de Gironcoli, S.; Baroni, S.; Kern, K. *Angew. Chem., Int. Ed.* **2005**, *44*, 6142−6145.
(36) Perdew, J. P.; Burke, K.; Ernzerhof, M. *Phys. Rev. Lett.* **1996**, *77*, 3865−3868.
(37) Vanderbilt, D. *Phys. Rev. B* **1990**, *41*, 7892−7895.
(38) Giannozzi, P.; Baroni, S.; Bonini, N.; Calandra, M.; Car, R.; Cavazzoni, C.; Ceresoli, D.; Chiarotti, G. L.; Cococcioni, M.; Dabo, I.; et al. *J. Phys.: Condens. Matter* **2009**, *21*, 395502.
(39) Monkhorst, H. J.; Pack, J. D. *Phys. Rev. B* **1976**, *13*, 5188−5192.
(40) Tersoff, J.; Hamann, D. R. *Phys. Rev. Lett.* **1983**, *50*, 1998−2001.
(41) Perry, C. C.; Haq, S.; Frederick, B. G.; Richardson, N. V. *Surf. Sci.* **1998**, *409*, 512−520.
(42) Lin, N.; Payer, D.; Dmitriev, A.; Strunskus, T.; Woll, C.; Barth, J. V.; Kern, K. *Angew. Chem., Int. Ed.* **2005**, *44*, 1488−1491.
(43) Ge, Y.; Adler, H.; Theertham, A.; Kesmodel, L. L.; Tait, S. L. *Langmuir* **2010**, *26*, 16325−16329.
(44) Mark, A. G.; Forster, M.; Raval, R. *ChemPhysChem* **2011**, *12*, 1474−1480.
(45) Schnadt, J.; Xu, W.; Vang, R. T.; Knudsen, J.; Li, Z.; Laegsgaard, E.; Besenbacher, F. *Nano Res.* **2010**, *3*, 459−471.
(46) Ruben, M. *Angew. Chem., Int. Ed.* **2005**, *44*, 1594−1596.
(47) Lin, N.; Stepanow, S.; Ruben, M.; Barth, J. V. In *Templates in Chemistry III*; Broekmann, P., Dötz, K.-H., Schalley, C. A., Eds.; Springer-Verlag: Berlin, Germany, 2009; Vol. *287*, pp 1−44.
(48) Kley, C. S.; Cechal, J.; Kumagai, T.; Schramm, F.; Ruben, M.; Stepanow, S.; Kern, K. *J. Am. Chem. Soc.* **2012**, *134*, 6072−6075.
(49) Tait, S. L.; Wang, Y.; Costantini, G.; Lin, N.; Baraldi, A.; Esch, F.; Petaccia, L.; Lizzit, S.; Kern, K. *J. Am. Chem. Soc.* **2008**, *130*, 2108−2113.
(50) Kuhnle, A.; Molina, L. M.; Linderoth, T. R.; Hammer, B.; Besenbacher, F. *Phys. Rev. Lett.* **2004**, *93*, 86101.
(51) Jeffrey; A. G. *An Introduction to Hydrogen Bonding*; Oxford University Press: Oxford, U.K., 1997.
(52) Steiner, T. *Angew. Chem., Int. Ed.* **2002**, *41*, 48−76.
(53) Wang, Y.; Fabris, S.; White, T. W.; Pagliuca, F.; Moras, P.; Papagno, M.; Topwal, D.; Sheverdyaeva, P.; Carbone, C.; Lingenfelder, M.; et al. *Chem. Commun.* **2012**, *48*, 534−536.
(54) Ndongmouo, U. T.; Hontinfinde, F.; Ferrando, R. *Phys. Rev. B* **2005**, *72*, 115412.
(55) Videcoq, A.; Hontinfinde, F.; Ferrando, R. *Surf. Sci.* **2002**, *515*, 575−587.
(56) De Giorgi, C.; Aihemaiti, P.; de Mongeot, F. B.; Boragno, C.; Ferrando, R.; Valbusa, U. *Surf. Sci.* **2001**, *487*, 49−54.